

# Spin-Flop Switching and Memory in a Molecular Conductor

Mitsuhiko Maesato,<sup>\*,†</sup> Tomohito Kawashima,<sup>†</sup> Yoshitomo Furushima,<sup>†</sup> Gunzi Saito,<sup>†,§</sup> Hiroshi Kitagawa,<sup>†,#</sup> Takashi Shirahata,<sup>‡,⊥</sup> Megumi Kibune,<sup>‡</sup> and Tatsuro Imakubo<sup>‡,||</sup>

<sup>†</sup>Division of Chemistry, Graduate School of Science, Kyoto University, Kitashirakawa Oiwake-cho, Sakyo-ku, Kyoto 606-8502, Japan

<sup>‡</sup>Imakubo Initiative Research Unit, RIKEN, 2-1 Hirosawa, Wako, Saitama 351-0198, Japan

<sup>#</sup>JST-CREST, Sanban-cho 5, Chiyoda-ku, Tokyo 102-0075, Japan

**S** Supporting Information

**ABSTRACT:** We report the first observation of spin-flop-induced sharp positive magnetoresistance as large as 100% and nonvolatile magnetoresistive memory in a  $\pi$ -d hybrid molecular conductor, (DIETSe)<sub>2</sub>FeCl<sub>4</sub> [DIETSe = diiodo(ethylenedithio)tetraselenafulvalene]. The unprecedented magnetotransport phenomena originate from the coexistence of the spin density wave (SDW) of the quasi-one-dimensional (Q1D)  $\pi$  electrons and the antiferromagnetic order of d-electron spins, indicating the interplay between the electronic instability of Q1D  $\pi$  electrons and local moments of antiferromagnetic d-electron spins. These findings offer new possibilities in molecular electronics/spintronics.

Magnetic conductors having a giant response to external stimuli have attracted much attention because of the fundamental interest in the mutual interaction between magnetism and conductivity and also practical applications, such as magnetic sensors, memories and spintronic devices.<sup>1</sup> For example, giant magnetoresistance (MR) and colossal MR have been extensively studied in inorganic alloys and oxides.<sup>2</sup> In contrast, molecular materials normally have weak spin-charge interaction; however, they are advantageous in terms of flexibility, low weight, small-size integration under mild conditions, weak spin-orbit interaction, and a wide variety of freedom in material design.<sup>3</sup>

A promising approach for the research on magnetic molecular conductors is to couple magnetism and conductivity by introducing inorganic magnetic species into organic conducting materials, and a number of dual-functional organic/inorganic hybrid materials have been developed.<sup>4</sup> An example of such a robustly coupled material is the quasi-two-dimensional (Q2D) conductor  $\lambda$ -(BETS)<sub>2</sub>FeCl<sub>4</sub> having magnetic-field-induced superconductivity,<sup>5</sup> where BETS denotes bis(ethylenedithio)tetraselenafulvalene and serves as a reservoir of  $\pi$  electrons. The Q2D nature of  $\pi$  electrons is advantageous in obtaining a stable metal<sup>6</sup> or superconductor<sup>7</sup> with magnetic ions. However, such stable electronic states would often be unsusceptible to the magnetic transition of incorporated spins.<sup>6</sup>

Reducing the dimensionality further to quasi-one dimension opens up a fascinating world where electrical conduction is highly susceptible to electron-electron and electron-phonon interactions. We have focused our attention on a spin density wave (SDW) of quasi-one-dimensional (Q1D)  $\pi$  electrons,

because it has been considered to couple with the antiferromagnetic (AF) order of d-electron spins via  $\pi$ -d interaction.<sup>8</sup> Among Q1D  $\pi$ -d conductors, (DIETSe)<sub>2</sub>FeCl<sub>4</sub> [DIETSe = diiodo(ethylenedithio)tetraselenafulvalene] has high conductivity down to low temperature because of enhanced intermolecular interactions due to the presence of heavy Se atoms in the inner tetraselenafulvalene (TSeF) skeleton (Figure 1a).<sup>9</sup> (DIETSe)<sub>2</sub>FeCl<sub>4</sub> also shows a clear

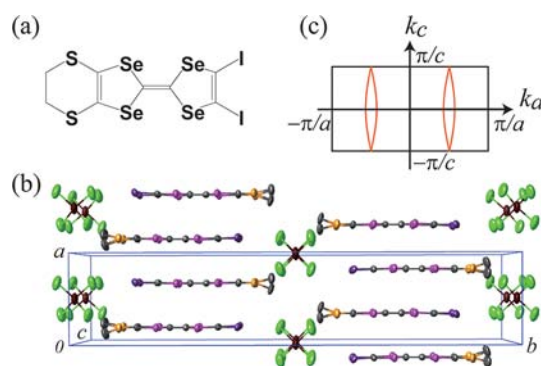


**Figure 1.** (a) Molecular structure of DIETSe. (b) Crystal structure of (DIETSe)<sub>2</sub>FeCl<sub>4</sub> viewed along the *c*-axis; DIETSe molecules only at (0, 0, 1/2) sites are shown. (c) Calculated Fermi surfaces in the *k<sub>a</sub>-k<sub>c</sub>* plane; the square area is the first Brillouin zone.

metal-insulator transition, followed by an AF transition of d-electron spins. Therefore, SDW and AF orders coexist in the ground state. The cooperative and/or competing effects of these symmetry-broken ground states can give rise to a clear and large response to external stimuli.

In this paper, we first report spin-flop-induced sharp positive MR and nonvolatile memory in a molecular crystal, (DIETSe)<sub>2</sub>FeCl<sub>4</sub>. We demonstrate that the electronic instability inherent to low-dimensional metals can be controlled by incorporated spins and external stimuli, providing a new path for the development of multifunctional molecular materials.

The DIETSe molecule was synthesized as described in the literature.<sup>10</sup> Elongated plate-like single crystals of (DIETSe)<sub>2</sub>MCl<sub>4</sub> [M = Fe, Ga] were prepared by electrochemical oxidation using Pt electrodes.<sup>9</sup> The good quality of the molecule and crystals was confirmed by elemental analysis

Received: August 26, 2012

Published: October 7, 2012

and X-ray diffraction. We extended our previous brief high-pressure experiment that provided results for the *b*-axis resistance down to 1.5 K<sup>11</sup> and obtained results down to 0.6 K in the present work. The detailed pressure–temperature phase diagrams were mapped out using an in situ pressure calibration. The details of physical property measurements are described in the Supporting Information (SI).

The (DIETSe)<sub>2</sub>MCl<sub>4</sub> [M = Fe, Ga] salts are isostructural to each other, having almost the same lattice parameters.<sup>9</sup> Fe<sup>3+</sup> has localized d-electron spins of high spin state (*S* = 5/2), while Ga<sup>3+</sup> is nonmagnetic (*S* = 0). Therefore, the Ga salt is a good reference material with which to clarify the nature of itinerant  $\pi$  electrons at DIETSe sites. Figure 1b shows the crystal structure of (DIETSe)<sub>2</sub>MCl<sub>4</sub> [M = Fe, Ga].<sup>9</sup> The planar DIETSe molecules stack uniformly, head-to-tail, along the crystallographic *a*-axis and form conduction columns. Band structure calculations predicted a highly 1D three-quarter-filled band with a Q1D Fermi surface (Figure 1c).<sup>9</sup> At ambient pressure, both salts are metallic down to about 12 K, below which the resistance increases with decreasing temperature.<sup>9</sup> The semi-conducting behavior below 12 K is attributable to an SDW transition due to nesting instability of the Q1D Fermi surface, as confirmed by a <sup>77</sup>Se nuclear magnetic resonance (NMR) study of the Ga salt.<sup>12</sup> The shape of the NMR spectra in the low-temperature phase is characteristic of an incommensurate SDW (ICSDW).<sup>12</sup>

To control the electronic states, we applied hydrostatic pressure to the crystals. Transport properties under a variety of hydrostatic pressures are shown in Figure 2 and in Figure S1 for

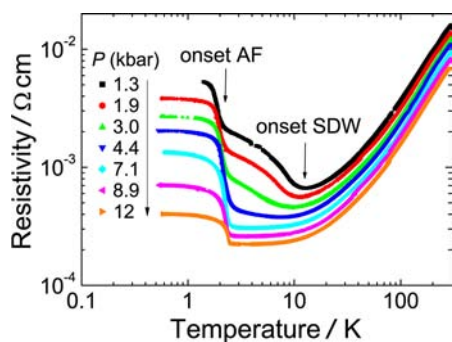


**Figure 2.** Temperature dependence of the electrical resistivity of (DIETSe)<sub>2</sub>FeCl<sub>4</sub> under various pressures.

Fe and Ga salts, respectively. Hydrostatic pressure monotonically suppresses the SDW transition in both salts, indicating suppression of nesting instability in the Fermi surface due to increased Fermi-surface warping.<sup>13</sup> Besides the SDW transition, the Fe salt has an additional anomaly in the temperature dependence of electrical resistivity below about 2.5 K, which corresponds to the AF transition temperature of Fe<sup>3+</sup> (*S* = 5/2) spins.<sup>9</sup> The large change in resistivity indicates an additional charge gap induced by the AF order. Because of the 2:1 composition, when there are alternating up- and down-spin sublattices of Fe<sup>3+</sup> along the *a*-axis,  $2k_F$  ( $= \pi/2a$ ) periodic modulation of the local moment appears. Thus, the  $2k_F$  AF order of Fe<sup>3+</sup> (*S* = 5/2) spins can induce an additional charge gap. We also note that such an additional anomaly is absent in the nonmagnetic Ga salt (Figure S1). The temperature–pressure phase diagram of (DIETSe)<sub>2</sub>FeCl<sub>4</sub> depicted in Figure 3 is similar to that of the Ga salt (Figure S2) except for the Néel temperatures *T*<sub>N</sub> of the d-electron spins, which are absent in the

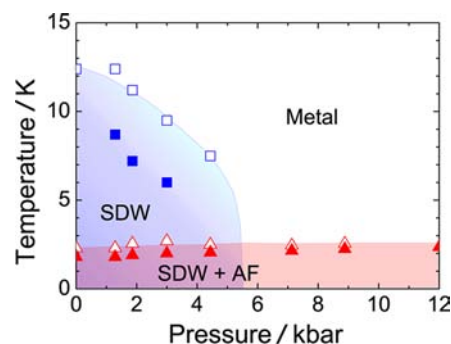


**Figure 3.** Temperature–pressure phase diagram of (DIETSe)<sub>2</sub>FeCl<sub>4</sub>. Open blue squares: the onset SDW transition temperature, where the resistivity is a minimum. Solid blue squares: the temperature at which  $d \ln(\rho)/d(1/T)$  has a peak, corresponding to the long-range ordering temperature of SDW *T*<sub>SDW</sub>. Open red triangles: onset AF transition temperature. Solid red triangles: the temperature at which  $d \ln(\rho)/d(1/T)$  has a peak, corresponding to the long-range AF ordering temperature *T*<sub>N</sub>.

latter. These results decisively confirm that the electronic states of  $\pi$  electrons are essentially the same for the two salts. For the Ga salt, the ICSDW state is completely suppressed above the critical pressure *P*<sub>c</sub> of about 6.5 kbar, recovering normal metallic behavior at 6.9 kbar (Figure S1). In contrast, for the Fe salt, the resistivity still increases below *T*<sub>N</sub> even above *P*<sub>c</sub> of about 5.5 kbar, indicating the partial gap at the Fermi energy induced by the  $2k_F$  AF order of Fe<sup>3+</sup> spins.

Figure 4a shows the magnetic-field dependence of the magnetic torque of (DIETSe)<sub>2</sub>FeCl<sub>4</sub> measured using a piezoresistive microcantilever. Under the magnetic field along the *b*-axis, a spin-flop transition of Fe<sup>3+</sup> (*S* = 5/2) spins is

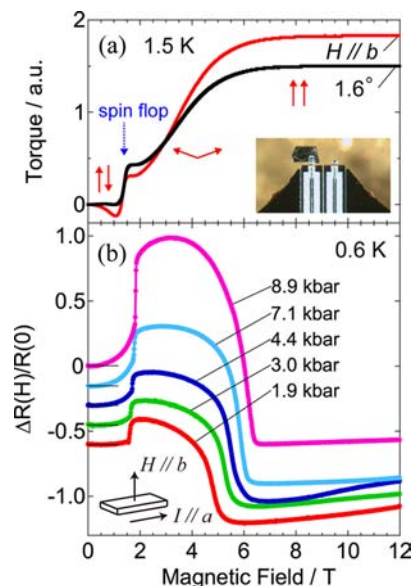


**Figure 4.** Correlation between magnetism and resistivity in (DIETSe)<sub>2</sub>FeCl<sub>4</sub>. (a) Magnetic torque at 1.5 K under the magnetic field applied along the *b*-axis (red points) and tilted 1.6° from the *b*-axis to the *c*-axis (black points). Red arrows show the relative orientation of Fe<sup>3+</sup> (*S* = 5/2) spins. The inset is a picture of a tiny single crystal on a piezoresistive microcantilever. (b) Magneto-resistance change at 0.6 K as a function of the magnetic field applied along the *b*-axis for several pressures. The data except for those for 8.9 kbar are shifted downward for clarity.

observed at 1.5 T and 1.5 K. Interestingly, we found that the spin flop, which is a first-order spin reorientation transition, strongly alters the conductivity in  $(\text{DIETSe})_2\text{FeCl}_4$ . Figure 4b shows the magnetic-field dependence of MR change,  $\Delta R(H)/R(0) = [R(H) - R(0)]/R(0)$ , under a variety of pressures. We observed a steep step-like increase in MR just above the spin-flop field.  $\Delta R(H)/R(0)$  increases with increasing pressure and reaches 100% at 8.9 kbar. This is unambiguous evidence of spin–charge-coupled ‘electrical switching’. Such a steep and positive (as opposed to negative) change for a weak magnetic field is an unforeseen peculiarity in  $\pi$ -d systems. In magnetic molecular conductors, negative MR is a common characteristic as has been observed at the boundary between a canted AF phase and a paramagnetic phase in Q2D  $\pi$ -d conductors.<sup>14</sup> Besides the negative MR, Q1D  $\pi$ -d conductors show a dip-like anomaly in MR associated with a spin-flop transition.<sup>8,15</sup> However, as far as we know, the step-like very steep and positive MR due to spin flop has never been observed in molecular conductors. We also note that it does not require the application of a strong magnetic field, in marked contrast to giant negative MR ( $\sim 18$  T) in phthalocyanine salt<sup>16</sup> and magnetic-field-induced superconductivity ( $\sim 17$  T) in BETS salt.<sup>5</sup> The positive MR above the spin-flop transition may be explained by enhancement of the charge gap or scattering due to reorientation of AF moments.

As the magnetic field strengthens, MR is gradually suppressed until about 6 T because the canted d-electron spins gradually polarize along the magnetic-field direction. As is evident in Figure 4a, the magnetic moment of d-electron spins becomes saturated above about 6 T, where the additional charge gap is suppressed because the  $2k_{\text{F}}$  periodic modulation of the Fe moments no longer occurs.

Remarkably, the MR shows irreversible hysteresis at low pressures below  $P_c$ . In Figure 5a, the black points show MR during the initial increase in the magnetic field; the red points show MR during down-sweep of the field below 3 T. Below the spin-flop field, the down-sweep MR is smaller than the up-sweep MR and never returns to its initial value after removal of the field, indicating irreversible hysteresis. Even if the field is applied again, the up-sweep MR remains small below the spin-flop field and merges into the initial MR above the spin-flop field. This is an intriguing peculiarity, which we call ‘spin-flop memory’, since the bulk resistance of the material is changed by the magnetic-field-induced spin-flop transition and the material indeed ‘remembers’ the transition. This is a new nonvolatile memory; the material can retain the stored information even after removal of the magnetic field. In other molecular conductors, unusual changes in MR due to the spin-flop transition<sup>8,15</sup> or transition from canted AF to paramagnetic phases<sup>14</sup> are rarely observed as mentioned above. However, the spin–charge-coupled ‘memory’ phenomenon has never been observed, to our knowledge.

We also found that the memory can be erased by increasing the temperature above  $T_{\text{N}}$ . A plot of the temperature dependence of resistivity (Figure 5b) shows initial cooling before (black points) and subsequent heating after (red points) the MR experiments described above. The low-resistivity ‘on’ state is observed during heating. Above  $T_{\text{N}}$ , the resistivity coincides with the initial value, indicating that memory is cleared.

At high pressures above  $P_c$ , this memory phenomenon is not observed (Figure S3), indicating that the coexistence of ICSDW and commensurate antiferromagnetism is important

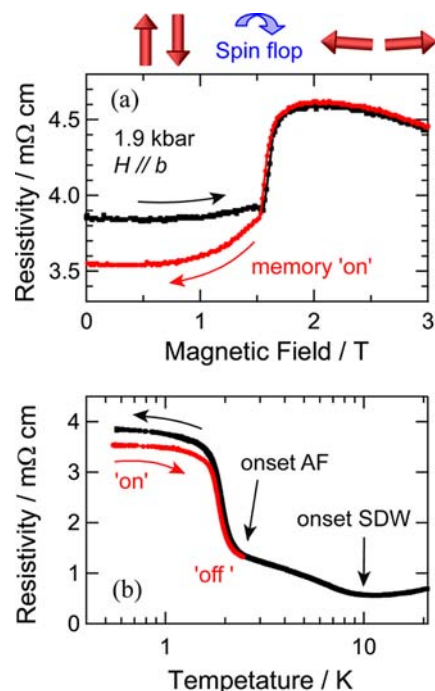


**Figure 5.** Spin-flop-induced magnetoresistive memory in  $(\text{DIETSe})_2\text{FeCl}_4$ . (a) Magnetoresistance at 0.6 K as a function of the magnetic field applied along the  $b$ -axis at 1.9 kbar. Black points: data taken during the initial strengthening of the magnetic field. Red points: data taken during the down-sweep of the magnetic field from 3 T. (b) Temperature dependence of resistivity before (black points) and after (red points) the MR study shown in (a). The low-resistivity ‘on’ state returns to the initial ‘off’ state upon heating above  $T_{\text{N}}$ .

to this phenomenon. We note that the AF order of d-electron spins should be commensurate to the lattice, while the wave vector of the 12 K SDW is determined by the optimum nesting vector of the Fermi surface and is most probably incommensurate, according to the NMR experiments of Ga salt.<sup>12</sup> Thus, the wave vectors should differ from one another.

It is difficult to describe precisely the observed anomalous MR, especially the memory phenomenon, because it involves a complicated scattering mechanism that may be affected by field-induced reconfigurations of AF domains. Besides the domain wall scattering, we suggest a possibility of field-induced incommensurate–commensurate transition, i.e., the lock-in transition of the SDW. The reorientation of AF d-electron spins in the spin-flop field may induce a lock-in transition of the SDW. The spin-flop-induced lock-in state is considered to be a metastable state pinned by the commensurate AF potential and might survive even if the external magnetic field is turned off. However, further investigations are required to clarify the origin of the memory phenomenon.

In conclusion,  $(\text{DIETSe})_2\text{FeCl}_4$  is the first example of a molecular conductor exhibiting a spin-flop-induced electrical switching and nonvolatile memory due to the interplay between SDW instability of the Q1D metal and periodic AF modulation of incorporated Fe spins. This material could be a prototypical example of multifunctional hybrid materials in which cooperative and/or competing order parameters of two sublattices can be used to manipulate both spin and charge degrees of freedom, simultaneously.



**■ ASSOCIATED CONTENT****📄 Supporting Information**

Experimental details of transport and magnetic torque measurements, transport properties, the temperature–pressure phase diagram of  $(\text{DIETSe})_2\text{GaCl}_4$ , and reversible MR of  $(\text{DIETSe})_2\text{FeCl}_4$  above the critical pressure. This material is available free of charge via the Internet at <http://pubs.acs.org>.

**■ AUTHOR INFORMATION****Corresponding Author**

maesato@kuchem.kyoto-u.ac.jp

**Present Addresses**

<sup>§</sup>Faculty of Agriculture, Meijyo University, 1–501 Shiogamaguchi, Tempaku-ku, Nagoya 468–8502, Japan

<sup>†</sup>Department of Applied Chemistry, Ehime University, 3 Bunkyo-cho, Matsuyama, Ehime 790–8577, Japan

<sup>‡</sup>Department of Materials Science and Technology, Nagaoka University of Technology, 1603–1 Kamitomioka, Nagaoka, Niigata 940–2188, Japan

**Notes**

The authors declare no competing financial interests.

**■ ACKNOWLEDGMENTS**

We thank C. Michioka, Y. Itoh, and K. Yoshimura for carrying out NMR experiments and holding discussions. This work was in part supported by Grants-in-Aid for the Global COE Program ‘International Center for Integrated Research and Advanced Education in Materials Science’ and Scientific Research on Innovative Areas (20110006) from MEXT, Japan and Grants-in-Aid for Young Scientists (B) (22740226) and Scientific Research (S) (23225005) from JSPS.

**■ REFERENCES**

- (1) (a) Wolf, S. A.; Awschalom, D. D.; Buhrman, R. A.; Daughton, J. M.; von Molnár, S.; Roukes, M. L.; Chtchelkanova, A. Y.; Treger, D. M. *Science* **2001**, *294*, 1488. (b) Chappert, C.; Fert, A.; Nguyen Van Dau, F. *Nat. Mater.* **2007**, *6*, 813.
- (2) (a) Baibich, M. N.; Broto, J. M.; Fert, A.; Nguyen Van Dau, F.; Petroff, F.; Etienne, P.; Creuzet, G.; Friederich, A.; Chazelas, J. *Phys. Rev. Lett.* **1988**, *61*, 2472. (b) Binasch, G.; Grünberg, P.; Saurenbach, F.; Zinn, W. *Phys. Rev. B* **1989**, *39*, 4828. (c) Jin, S.; Tiefel, T. H.; McCormack, M.; Fastnacht, R. A.; Ramesh, R.; Chen, J. H. *Science* **1994**, *264*, 413. (d) Ramirez, A. P. *J. Phys.: Condens. Matter* **1997**, *9*, 8171.
- (3) (a) Saito, G.; Wudl, F.; Haddon, R. C.; Tanigaki, K.; Enoki, T.; Katz, H. E.; Maesato, M., Eds. *Multifunctional Conducting Molecular Materials*; RSC Publishing: Cambridge, 2007. (b) Kippelen, B.; Brédas, J. L. *Energy Environ. Sci* **2009**, *2*, 251. (c) Sanvito, S. *Chem. Soc. Rev.* **2011**, *40*, 3336. (d) Shiraishi, M.; Ikoma, T. *Physica E* **2011**, *43*, 1295.
- (4) (a) Coronado, E.; Day, P. *Chem. Rev.* **2004**, *104*, 5419. (b) Enoki, T.; Miyazaki, A. *Chem. Rev.* **2004**, *104*, 5449. (c) Kobayashi, H.; Cui, H. B.; Kobayashi, A. *Chem. Rev.* **2004**, *104*, 5265. (d) Sugimoto, T.; Fujiwara, H.; Noguchi, S.; Murata, K. *Sci. Technol. Adv. Mater.* **2009**, *10*, 024302.
- (5) Uji, S.; Shinagawa, H.; Terashima, T.; Yakabe, T.; Terai, Y.; Tokumoto, M.; Kobayashi, A.; Tanaka, H.; Kobayashi, H. *Nature* **2001**, *410*, 908.
- (6) Coronado, E.; Galán-Mascarós, J. R.; Gómez-García, C. J.; Laukhin, V. *Nature* **2000**, *408*, 447.
- (7) Kurmoo, M.; Graham, A. W.; Day, P.; Coles, S. J.; Hursthouse, M. B.; Caulfield, J. L.; Singleton, J.; Pratt, F. L.; Hayes, W. *J. Am. Chem. Soc.* **1995**, *117*, 12209.
- (8) (a) Enomoto, K.; Yamaura, J.; Miyazaki, A.; Enoki, T. *Bull. Chem. Soc. Jpn.* **2003**, *76*, 945. (b) Okabe, K.; Yamaura, J.; Miyazaki, A.; Enoki, T. *J. Phys. Soc. Jpn.* **2005**, *74*, 1508. (c) Nishijo, J.; Miyazaki, A.

- Enoki, T. *Inorg. Chem.* **2005**, *44*, 2493. (d) Enoki, T.; Okabe, K.; Miyazaki, A. In *Multifunctional Conducting Molecular Materials*; Saito, G., Wudl, F., Haddon, R. C., Tanigaki, K., Enoki, T., Katz, H. E., Maesato, M., Eds.; RSC Publishing: Cambridge, 2007, 153–160. (e) Miyazaki, A.; Yamazaki, H.; Aimatsu, M.; Enoki, T.; Watanabe, R.; Ogura, E.; Kuwatani, Y.; Iyoda, M. *Inorg. Chem.* **2007**, *46*, 3353.
- (9) Shirahata, T.; Kibune, M.; Maesato, M.; Kawashima, T.; Saito, G.; Imakubo, T. *J. Mater. Chem.* **2006**, *16*, 3381.
- (10) Imakubo, T.; Shirahata, T. *Chem. Commun.* **2003**, 1940–1941.
- (11) Maesato, M.; Kawashima, T.; Saito, G.; Shirahata, T.; Kibune, M.; Imakubo, T. *Mol. Cryst. Liq. Cryst.* **2006**, *455*, 123.
- (12) Michioka, C.; Itoh, Y.; Yoshimura, K.; Furushima, T.; Maesato, M.; Saito, G.; Shirahata, T.; Kibune, M.; Imakubo, T. *J. Phys.: Conf. Ser.* **2009**, *150*, 042124.
- (13) Yamaji, K. *J. Phys. Soc. Jpn.* **1982**, *51*, 2787.
- (14) (a) Balicas, L. *Solid State Commun.* **2000**, *116*, 557. (b) Uji, S.; Shinagawa, H.; Terai, Y.; Yakabe, T.; Terakura, C.; Terashima, T.; Balicas, L.; Brooks, J. S.; Ojima, E.; Fujiwara, H.; Kobayashi, H.; Kobayashi, A.; Tokumoto, M. *Physica B* **2001**, *298*, 557. (c) Choi, E. S.; Graf, D.; Brooks, J. S.; Yamada, J.; Akutsu, H.; Kikuchi, K.; Tokumoto, M. *Phys. Rev. B* **2004**, *70*, 024517. (d) Jo, Y. J.; Kang, H.; Kang, W.; Uji, S.; Terashima, T.; Tanaka, T.; Tokumoto, M.; Kobayashi, A.; Kobayashi, H. *Phys. Rev. B* **2006**, *73*, 214532.
- (15) (a) Hayashi, T.; Xiao, X.; Fujiwara, H.; Sugimoto, T.; Nakazumi, H.; Noguchi, S.; Fujimoto, T.; Yasuzuka, S.; Yoshino, H.; Murata, K.; Mori, T.; Aruga-Katori, H. *J. Am. Chem. Soc.* **2006**, *128*, 11746. (b) Fujimoto, T.; Yasuzuka, S.; Yokogawa, K.; Yoshino, H.; Hayashi, T.; Fujiwara, H.; Sugimoto, T.; Murata, K. *J. Phys. Soc. Jpn.* **2008**, *77*, 014704. (c) Fujimoto, T.; Hayashi, T.; Sugimoto, T.; Yoshino, H.; Murata, K. *J. Phys. Soc. Jpn.* **2009**, *78*, 014710.
- (16) Hanasaki, N.; Tajima, H.; Matsuda, M.; Naito, T.; Inabe, T. *Phys. Rev. B* **2000**, *62*, 5839 (2000).